Plasmonic Enhanced Photodetectors for Near Infra-red Light Detection

D. Giubertoni[1*], G. Paternoster[1], F. Acerbi[1], X. Borrisé[2], A. Cian[1], A. Filippi[1,3], A. Gola[1], A. Guerrero[4], F. Perez Murano[4], F. Romanato[3], E. Scattolo[1,5] and P. Bellutti[1]

[1] Center for Materials and Microsystems, Fondazione Bruno Kessler, Trento, Italy
[2] Institut Català de Nanociència i Nanotecnologia, Bellaterra (Barcelona), Spain
[3] Department of Physics and Astronomy "G. Galilei", University of Padua, Padua, Italy
[4] Instituto de Microelectrónica de Barcelona – (IMB-CNM, CSIC), Bellaterra (Barcelona), Spain
[5] Libera Università Di Bolzano, Bozen, Italy

* Corresponding author: giuberto@fbk.eu

Abstract - **Silicon based single photon avalanche diodes (SPAD) are able to detect single photons in the visible part of the spectrum with high detection efficiency and high timing resolution. They also provide both single-photon sensitivity and fast responsivity in large-area detectors if arranged in extended arrays as Silicon Photomultipliers (SiPM). However, in applications exploiting near infrared light like light detection and ranging (LiDAR), the detector performance is hindered by the limited Si absorption coefficient. The latter implies absorption depths much larger than the typical active thickness of these devices (10-100 µm against few micrometers) resulting in a quantum efficiency (QE) too low for most of the previous applications. The exploitation of Surface Plasmon Polaritrons (SPP) can convert light in highly-confined modes and enhance the absorption of NIR photons. In this contribution, the first results on the integration of plasmonics nanostructures on thin silicon photodiodes are reported. Electro-optical measurements were carried out and the QE has been measured in the full 400-1100 nm spectrum. The resulting QE on the first prototypes is higher than 7% at 950 nm, an enhancement of about 45% with respect to the reference structure, paving the way for the application of metallic nanograting to SPADs and SiPMs devices.**

Keywords - SPAD; SiPM; surface plasmon polaritrons; Si photodetector; plasmonics.

I. INTRODUCTION

The possibility to detect and accurately measure single photons is a crucial step in a wide range of recent technological applications and scientific experiments. Silicon based single photon avalanche diodes (SPADs) are able to provide both high sensitivity and extremely fast single-photon detection. Furthermore, if arranged in extended arrays they can be the building block of Silicon Photomultipliers (SiPM), providing single-photon sensitivity in large-area detectors [1]. Some emerging applications rely on the photon detection in the red and NIR spectral range, e.g. LiDAR (at 850 - 950 nm wavelengths), NIR spectroscopy, quantum computation, and the detection of light from NIR emitting scintillators. Nowadays, the Photon Detection Efficiency (PDE) of standard SiPMs is strongly limited in the NIR spectral range due to the relatively low Si absorption coefficient [2]. The latter implies absorption depths much larger than the typical active thickness of ("thin") Si SPADs, i.e. few micrometers for the latter against ~18 µm absorption depth at 850 nm and ~150 µm at 1000 nm. Therefore, the detection efficiency is still considered low for most of the previously cited applications.

Latest developments in nanophotonics and plasmonics showed that nanostructured metallic surfaces supporting Surface Plasmon Polaritrons (SPP) could be effectively used to shape light in highly-confined modes and enhance the absorption of NIR photons in thin or poor-absorbing materials like Silicon [3]. Some of these interesting surfaces are: i) 1- and 2-dimensional gratings; ii) bullseye structures; iii) nano-pillars and nano-holes arrays. Nanogratings made of noble metals are very promising structures, also considering the feasibility and the possible integration with SPAD and SiPM technologies, i.e. preserving all the advantages of a Si-based IC technology.

With the aim to investigate and validate the application of metallic nanostructures to SPAD and SiPM devices, in this work, we report on the integration of plasmonic nanostructures on state of art photodetectors (PDs). At the current stage of development, the test devices consist of conventional Silicon photodiodes instead of a proper SPAD, due to the simpler production and characterization procedures with respect to Geiger-mode operations. The photodiodes have been produced at the facility of Fondazione Bruno Kessler (Trento, Italy) by exploiting a custom CMOS-like microfabrication process similar to the one used for FBK-SiPM technology [4].

The produced PDs have been integrated with metal nanograting structures, fabricated directly on the top of the photodiodes by means of Electron Beam Lithography (EBL) followed by Silver evaporation and lift-off. Afterwards, the produced samples have been characterized in terms of Quantum Efficiency (QE) in the full 400-1100 nm spectrum. The paper is organized as follows: in the section II, the device structure and layout are presented

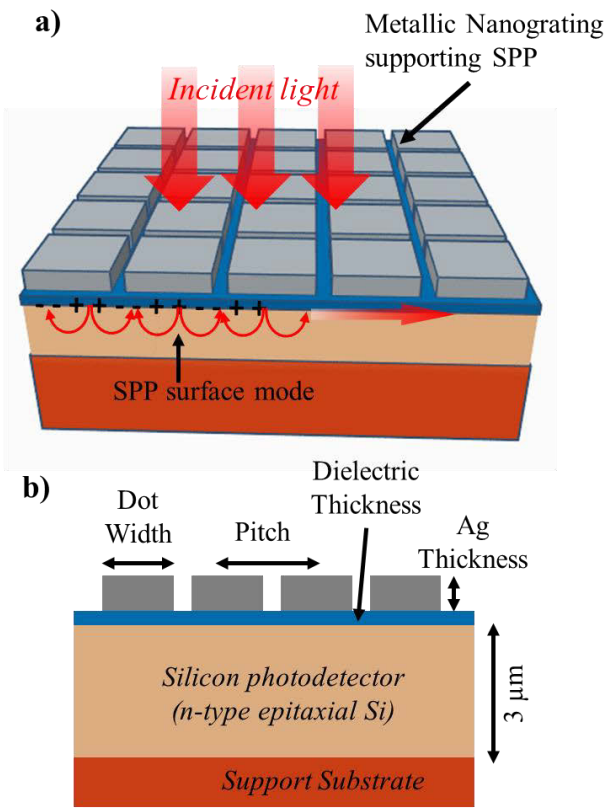

Figure 1. Proposed structure of Metal nanograting fabricated on the top of a Silicon photodiode passivated with a thin dielectric film (a); cross section of the same structure where the parameters optimized in the simulations are indicated (b).

together with the numerical methods used to simulate the optical response of the device; in section III, experimental methods and results from the micro- and nano-fabrication process are reported and discussed; section IV reports the electro-optical characterization of the first prototypes; the conclusions are included in the last section.

II. Device Design and Numerical Simulations

The proposed detector structure is presented in Fig.1, where a not-in-scale 3D sketch and a cross-section are shown. In this design, the silicon photodiode consists of a thin silicon slab (3 µm thick), which is the typical thickness used for SiPMs and SPAD production. The top detector surface is protected by a thin dielectric film (silicon nitride) with a twofold aim: i) to passivate the detector surface and reduce the surface recombination velocity; ii) to act as an optical coupling layer between the detector and the plasmonic nanograting. The latter requires that the dielectric layer thickness has to be precisely tuned, as its thickness and dielectric function define the SPP resonance wavelength. The metal grating supporting SPP is being fabricated directly on the top of the detector in order to lie very close to the active part of the sensor. The grating can be 2-dimensional (periodic "open" strips) or 3-dimensional (dots array, as represented in Fig. 1). In the first case, TM polarized light only excites

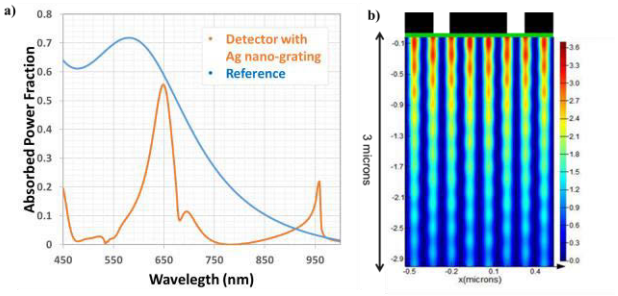

Figure 2. a) Simulated absorption in the 3 µm thick silicon detector with Ag nano-grating (orange solid line) and without (blue solid line); b) absorbed power density in the detector cross-section (a.u) at 952 nm.

SPP resonances as TE modes does not support surface plasmons. In the second case, 3-dimensional numerical simulations show that the same optical response of the 2-d grating appears for both TM and TE polarization, actually leading to a polarization-independent optical response.

In order to finely tune the detector design and estimate the grating optical performance, finite-difference time-domain simulations have been exploited, by using a commercial simulation engine (FDTD Lumerical software [5]). For simplicity, 2-dimensional gratings and TM polarized light have been simulated, while the simulation domain corresponds to a single strip with periodic boundary conditions at the edges. This model setup provides a low simulation time as well as the same level of accuracy obtained with 3-dimensional grating and not-polarized light source. The fraction of the absorbed power in a 3 µm thick Silicon sensitive region has been simulated in the range 450-1100 nm and used as optimization parameters. With Reference to Fig.1b the following parameters have been tuned with the aim of maximizing the absorbed power fraction in the silicon substrate at 952 nm: i) grating pitch; ii) Si_3N_4 thickness; iii) Ag thickness; iv) duty cycle (defined as the ratio between dot width and pitch). The most promising structure features a pitch of 530 nm, duty cycle of about 80%, ~100 nm thick Ag and a thin Si_3N_4 film < 15 nm. The absorbed power fraction as a function of wavelength with this set of parameters is represented in Fig. 2a (orange solid line) together with the absorption curve of 3 µm thick Silicon without Ag grating (blue solid line), used as reference. The simulated spectrum shows multiple absorption peaks that can be related to both plasmonic and hybrid opto-plasmonic resonances. In particular, at 950 nm, a narrow and asymmetrical absorption peak "Fano-like" is present, in correspondence of the Rayleigh singularity wavelength [6]. At that wavelength the absorption reaches the 25%, an eight-fold enhancement with respect to the reference. The physical interpretation of these resonance peaks goes beyond the scope of this paper and can be found in [7]. The map of the absorbed power density at 952 nm, corresponding to maximum of that absorption peak, is reported in Fig. 2b, where it is clearly visible the light confinement in the first micron due to excitation of the hybrid opto-plasmonic mode.

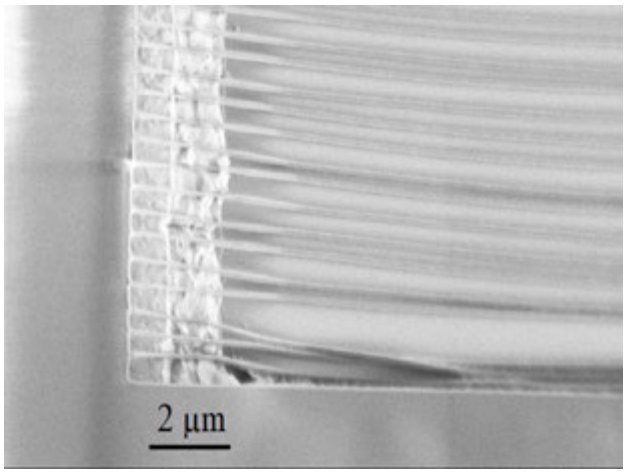

Figure 3. SEM planview of EBL exposed and developed stripe array on PMMA resist, near the edge of the PD. Design linewidth was 340 nm with 535 nm period.

III. MICRO- AND NANO-FABRICATION TECHNOLOGY

A. *Micro- fabrication of photodiodes*

The integration of Ag nanodots in direct contact with the detector top surface poses new challenges in both the micro- and nano-fabrication process, due to the presence of morphology and roughness in the photodiode surface, which hosts electrical contacts and metals for the diode biasing.

The manufacturing technology and the layout of the photodiode have been modified and optimized to host the nanostructure. The most critical parameter of the new diode design is the ultra-thin (< 15 nm) dielectric passivation layer, required in between the nanograting and the Silicon. Small diodes with different side (100 - 500 µm) were produced on a (3.5 ± 0.5) µm thick n-type epitaxial-Silicon wafers, while an ultra-shallow p-n junction has been formed by means of ion implantation. Both the substrate and the junction technology are similar to the one used in the FBK Near Ultra Violet, high-density (NUV-HD) SiPM technology [4], which features detection efficiency peaked at about 400 nm. Despite the target of NIR-wavelength applications, a shallow junction optimized for NUV light detection has been used because most of the plasmonic modes are typically confined in the first hundreds of nanometers from the detector surface.

B. *Nano-Fabrication of the plasmonic arrays*

The process chosen for the nano-fabrication of the dot array is based on positive-tone resist patterning, ultra-high vacuum metal evaporation and lift-off. The resist patterning was carried out by electron beam lithography (EBL) using a Raith150^{TWO} instrument. EBL provides adequate lateral nanometric resolution and flexibility on design parameters. Furthermore, the designed grating can be easily drawn on the surface of the PDs. In order to ensure a successful lift-off, a resist ~3 times thicker than the Ag layer is required. The final choice was to deposit PMMA 950k dilute in anisole (A7) by spin coating (4,500 rpm, 1 minute, curing at 180°C/ 1 minute), then developed with a 30 s dip in a MIBK:IPA 1:3 solution, stopping 30 s in IPA. EBL parameters (electron energy, intensity, dose of exposure) will be discussed in the next paragraphs.

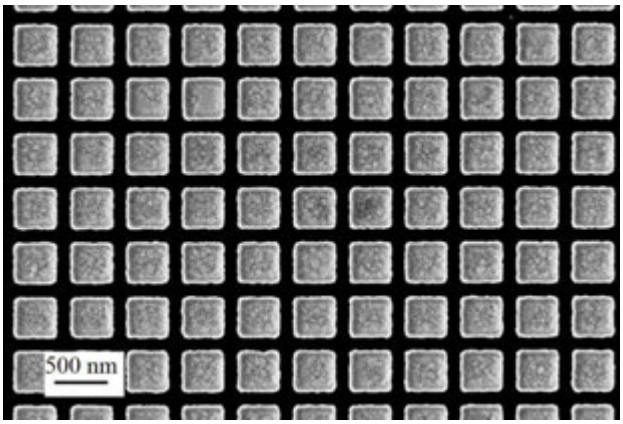

Figure 4. SEM planview of a nanosquare array produced on the surface of a PD with 11.0 nm of Si_3N_4 passivation. Design square size 400x400 nm with 535 nm period, Ag thickness 115 nm. EBL was carried out using a 10 kV/ ~20 pA beam, dose 120 µC/ cm^2.

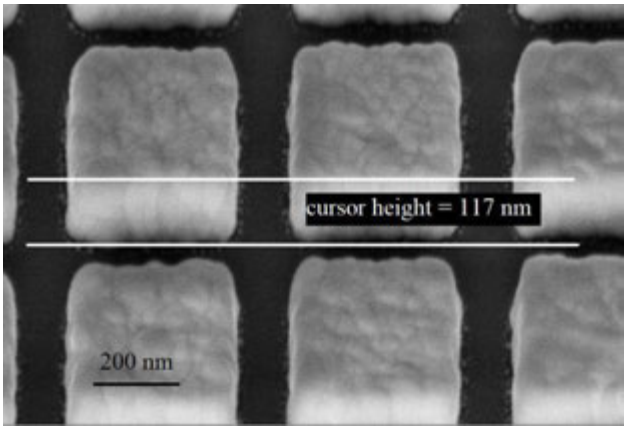

Figure 5. SEM image of the sample of Figure 3 with larger magnification and 45 ° tilt. The measured Ag thickness is 117 nm.

Ag evaporation was carried out in an e-beam evaporator. No adhesion layer was deposited before Ag evaporation to preserve the optical properties of the structures. Lift-off was carried out in acetone at 40 °C without any stirring given the absence of adhesion layers. In order to prevent the oxidation of the metallic pattern the devices were capped by spin coating a thin layer of PMMA resist (4% in Anisole, 4,500 rpm, 1 minute, curing at 180°C/ 1 minute) right after the lift-off process. This passivation allows also an easy opening of the electric contacts by EBL to connect the chip to the electro-optical characterization setup.

The required large duty cycle (up to 80%) implies that structures as wide as 430 nm need to be written by EBL with a period of 535 nm, i.e. leaving unexposed resist areas of only ~100 nm width. This patterning is hindered in this thick resist by the proximity effects, i.e. the unintentional exposure of resist by the electrons backscattered by the substrate. Proximity effects can produce a total pattern overexposure or also only a full exposure under the resist lines among stripes and dots, with possible collapse of the lines. Several combinations of EBL writing conditions were tested and best results were obtained using a 10 kV electron beam. Higher beam energy provided better lateral resolution but did not produce adequate undercuts for lift-off.

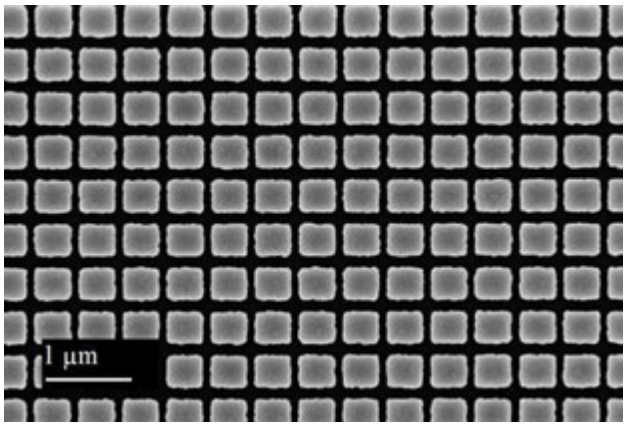

Figure 8. SEM planview of a nanosquare array produced on the surface of a PD with 12.5 nm of Si_3N_4 passivation. Design square size 350x350 nm with 535 nm period, Ag thickness 115 nm. EBL was carried out using a 10 kV/ ~200 pA beam, total dose 120 µC/ cm^2.

Two nano-arrays were tested: stripes and orthogonal array of squares, respectively. For the square arrays, period and duty cycle were always identical in x- and y-directions. Stripe arrays resulted impossible to integrate on the photodiode surface. An example of typical EBL outcome is reported in Figure 3, where the edge of a stripe array is shown. Stripe linewidth was 340 nm with 535 nm periodicity from design. EBL was carried out at low dose (70 µC/ cm^2) with a 10 kV/ ~200 pA electron beam. Even so, the unexposed resist lines among the stripes collapsed as clearly observed from the edge of the array. In general, the ~100 nm unexposed lines and their length (either 100 or 200 µm depending on the chosen PD) did not allow the stability of the resist wall. Therefore, lift-off could not succeed for this kind of design.

A different case was the nanosquare array design. Here the resist structure was somehow self-sustaining thanks to the cross-structure of the lines, and large duty cycles were achieved as reported in Figures 4 and 5 for a PD surface with 11 nm Si_3N_4 (design: 400x400 nm squares, 540 nm period; EBL dose 120 µC/cm^2). It is interesting to notice that these results were achievable only with low current electron beams (~20 pA). In fact, larger intensities of electron beam (~200 pA) resulted in rectangular instead of square shapes like observed in Figure 8, presumably because of some dynamical charging effects. For these reasons, all the samples for the electro-optically characterization were produced with the 10 kV/ 20 pA electron beam condition.

It is interesting to notice that no Ag dots were lost after lift-off despite the lack of an adhesion layer. Furthermore, the large thickness of evaporated Ag resulted in rather rough nanosquares in both planar and vertical directions, due to the polycrystalline nature of the evaporated Ag.

IV. Electro-Optical Characterization

A. Characterization Methods

In order to characterize the first detector prototypes, a custom setup was used. The light source is an unpolarized broadband halogen lamp connected to a monochromator that cover the visible and NIR light spectrum. The monochromator is provided with a variable slit which select the output spectrum width (± 3 nm 3σ). The device under test (DUT) is being mounted to a printed circuit

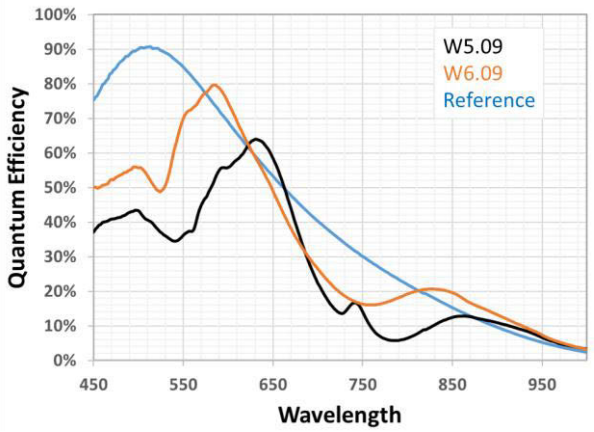

Figure 6. QE as a function of wavelentgh of the two PD with nanogratings (orange and black lines) and of the reference PD without nanograting (blue line).

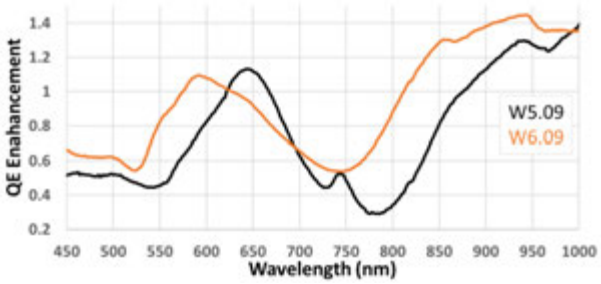

Figure 7. QE enahncement of the two samples with Ag nanograting with respect to the reference PD as a function of wavelentgh.

board (*PCB*) and wire-bonded in order to provide bias to PD. The packaged device is then mounted on a 3-axis stage for detector-beam centering. The actual incident power has been measured by means of a calibrated detector which was moved in place of the DUT during calibration. The PD is biased at 0 V and the photo-generated current is read by means of a semiconductor analyzer with a sensitivity of 1 pA. The measured photo-generated current, corrected for the dark current of the detector is used to calculate the external Quantum Efficiency (QE) of the devices.

B. Characterization Results

Two PD samples with different array geometries have been characterized together with a reference diode (without nano-grating) fabricated on the same silicon chip. The active area of PDs (fully covered by the nanodot array) is 200 x 200 µm^2. The two samples differ in terms of duty cycle of the nano-array and Si_3N_4 layer thickness, as shown in the Table I, which reports the nominal values of the main geometrical parameters of the samples.

TABLE I. Geometrical Parameters of the Samples

Sample ID	W5.09	W6.09	Reference
Grating Pitch	535 nm	536 nm	-
Duty Cycle	76 %	66 %	-
Si_3N_4 Thickness	11 nm	6.6 nm	11 nm
Ag Thickness	115 nm	115 nm	-

The experimental QE of both the PDs provided with dots-arrays (black and orange solid lines for W5.09 and W6.09, respectively) together with the reference diode (blue solid line) are reported in Fig. 6, while the ratio between the QE of the two PDs with dots-arrays and the QE of the reference diode are reported in Fig. 7. It is worth noting that the experimental QE reproduces the main features of the simulated absorption spectrum (orange curve in Fig. 2a). However, no sign of the narrow "Fano-like" peak predicted by the simulations at 950 nm can be found in the measurements, but a broader peak is present at shorter wavelengths (about 850 nm). Probably, the difference between simulated and measured QE in the NIR spectral region, seems to be mostly due to the difference of dielectric and metal thicknesses of the samples with respect to the optimal values suggested by numerical simulations. Deeper investigations are still ongoing and new samples will be soon available.

Even if the performance of the first prototypes are still far from the ideal case suggested by numerical simulation, the QE enhancement in the NIR region reaches the 45% at 950 nm in the case of the sample W6.09, a very remarkable result that pave the way for further optimizations.

V. CONCLUSION

The integration of silver nanosquare arrays supporting Surface Plasmon Polaritrons (SPP) increases the light absorption of NIR photons on Si photodiodes. In particular the plasmonic arrays can convert light in highly-confined modes reducing the NIR photons absorption depth to values comparable to the typical active regions of Si photodetectors. The first promising results of this approach have been here reported, showing a resulting QE higher than 7% at 950 nm, i.e. an enhancement of about 45% with respect to the reference structure, paving the way for the application of metallic nanograting to SPADs and SiPMs devices.

ACKNOWLEDGMENT

This project has received funding from the EU-H2020 research and innovation programme under Grant Agreement 777222 ATTRACT project "PlaSiPM" and under grant agreement No 654360 NFFA-Europe"

REFERENCES

[1] P. Buzhan et al., "Large area silicon photomultipliers: performance and applications," Nucl. Instrum. Methods Phys. Res. A,, vol. 567.1, pp. 78-82, 2006.

[2] F. Acerbi, G. Paternoster, A. Gola, N. Zorzi and C. Piemonte, "Silicon photomultipliers and single-photon avalanche diodes with enhanced NIR detection efficiency at FBK," Nucl. Instrum. Methods Phys. Res. A,vol. 912, pp. 309-314, 2018.

[3] P. Berini, Laser and Photonics Reviews, vol. 8.2, pp. 197-220, 2014, DOI: 10.1002/lpor.201300019

[4] C. Piemonte et al., "Performance of NUV-HD silicon photomultiplier technology, " IEEE Transactions on Electron Devices, vol. 63.3, pp. 1111-1116, 2016.

[5] Lumerical Inc. https://www.lumerical.com/products/.

[6] A. Hessel and A. A. Oliner,"A New Theory of Wood's Anomalies on Optical Gratings," Appl. Opt., vol. 4.10, pp. 1275-1297, 1965.

[7] A. Filippi, "Improving Silicon Photodetectors NIR Responsivity via Hybrid Opto-Plasmonic Resonances" PhD diss., Universita' degli Studi di Padova, 2020.